LUND UNIVERSITY

Numerical simulation of unsteady flow around a square two-dimensional cylinder

Sohankar, Ahmad; Davidson, Lars; Norberg, Christoffer

[Link to publication](#)

NUMERICAL SIMULATION OF UNSTEADY FLOW AROUND A SQUARE TWO-DIMENSIONAL CYLINDER

Ahmad Sohankar and Lars Davidson
Thermo and Fluid Dynamics
Chalmers University of Technology
Göteborg
Sweden

Christoffer Norberg
Division of Heat Transfer
University of Lund
Lund
Sweden

ABSTRACT

Calculations of two-dimensional unsteady flow around a quadratic two-dimensional cylinder at zero angle of attack are performed. The Reynolds numbers are low ($Re = 45$ - 250) so that the flow presumably is laminar. At $Re > 50$ a von Kármán vortex street with a well-defined shedding frequency is predicted. An incompressible SIMPLEC finite volume code employing non-staggered grid arrangement is used. A third-order QUICK scheme and a second-order Van Leer scheme are used for the convective terms. The time discretization is implicit and a second-order Crank-Nicolson scheme is employed. At $Re = 100$, the influence of the location of the inflow, outflow and side walls (blockage), respectively, is investigated. A number of quantities such as lift and drag coefficients and various surface pressure coefficients are presented.

NOMENCLATURE

In the following, unless otherwise stated, all dimensions are scaled with the side of the cylinder d, velocities with the constant upstream velocity U_∞, physical times with d/U_∞, fluid forces with d and the dynamic pressure of the upstream flow $\rho U_\infty^2/2$ and pressures with the dynamic and static pressure of the upstream flow ($C_p = 2(p - p_\infty)/\rho U_\infty^2$), respectively. Reynolds and Strouhal numbers are based on d and U_∞.

B	Blockage ($= d/H$)
C_D	Total drag coefficient
$C_{D'}$	RMS drag coefficient
C_{D_p}	Pressure drag coefficient
C_L	Total Lift coefficient
$C_{L'}$	RMS lift coefficient
C_{pb}	Base pressure coefficient at centerline
C_{ps}	Stagnation pressure coefficient at centerline
$C_{p,f}$	Surface averaged frontal side C_p
$C_{p,tb}$	Surface averaged top/bottom side C_p
H	Height of computational domain
L_r	Time mean length of recirculating region
Re	Reynolds number
St	Strouhal number
t	Non-dimensional time
U	Streamwise velocity
V	Cross stream velocity
X_d	Extent of domain downstream of body
X_u	Extent of domain upstream of body
Δt	Non-dimensional time step

INTRODUCTION

The subject of flow around slender bluff bodies is of relevance to many practical applications, e.g. chim-neys, tubular heat exchangers, offshore structures and pipelines, suspension bridges, towers, masts and wires. Under normal circumstances and when these structures are exposed to cross flow there is a massive separated region downstream of the body. Due to wake instabilities the phenomenon of vortex shedding usually develops (von Kármán vortex street). When scaled with the cross stream dimension of the body, the critical Reynolds number where the vortex shedding commences is of the order $Re_c = 50$. In the laminar régime, which usually persists up to Reynolds numbers of about 200 - 300, the vortex shedding is characterized by a very well-defined frequency. In addition to the engineering relevance of vortex shedding, e.g. in the fields of flow-induced sound and vibration, the study of bluff body wakes and its associated forces and wake frequencies is of great fundamental interest.

In recent years, the attention to flow around rectangular cylinders has accelerated. At low to moderate Reynolds numbers, such flows have been computed by e.g. Davis & Moore[1] Franke et al.[2], Okajima[4], Okajima et al.[5], Zaki et al.[8] and Kelkar & Patankar[3]. Davis & Moore, Franke et al. as well as Kelkar & Patankar use finite volume methods whereas Okajima et al. and Zaki et al. use finite differences. At Reynolds numbers relevant to this study, i.e. $Re \leq 250$, the only experimental results available in the open literature seems to be those of Okajima et al.[4-6] and Davis & Moore[1].

BOUNDARY CONDITIONS

The inlet is placed some body heights upstream of the body, see Fig. 1, where $U = 1$, $V = 0$ is prescribed. At the outlet, the U-velocity is calculated from global continuity together with a zero gradient boundary condition for both U and V. No-slip conditions are prescribed at the body surfaces ($U = V = 0$). At the upper and lower boundaries symmetry conditions simulating a frictionless wall are used ($V = \frac{\partial U}{\partial y} = 0$). The second normal derivative for the pressure is set to zero at all boundaries. The time-marching calculations are started with the fluid at rest, after which the inlet velocity is increased to unity in two time units by a sine function.

RESULTS AND DISCUSSION

At $Re = 100$, an extensive investigation of influence of time step, grid size and extent of the computation domain (Fig. 1) is presented. In these sensitivity studies, the RMS lift coefficient was found to be the most overall sensitive indicator. Finally, at $B = 5\%$, the influence of Reynolds number was investigated. All time
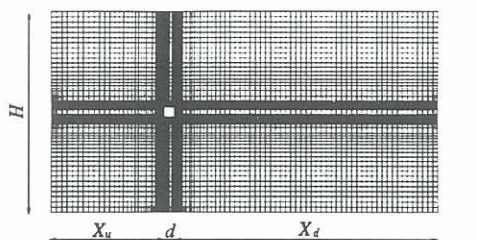
FIG. 1. THE 150×110 NON-UNIFORM GRID

FIG. 2. TIME AVERAGED PRESSURE
COEFFICIENT ALONG THE CENTERLINE

averages were calculated from the final time period i.e. in stationary flow condition. Strouhal numbers were calculated from the fluctuating lift.

Influence of Time Step and Grid

If too large values Δt are chosen, the phase as well as the amplitude accuracy will deteriorate. When considering both these aspects as well as the relatively long computer simulation times involved, it was finally decided to use the value $\Delta t = 0.025$. This value was also chosen by Franke & Rodi[2]. Decreasing the time step to 0.02 gave an increase of 1.5% in the RMS lift with negligible phase error. With a time step of $\Delta t = 0.05$ the RMS lift decreased by 11.5%.

Distribution of grid points in non-uniform grids, e.g. by the hyperbolic tangent and the hyperbolic sine functions, are discussed by Thompson et al.[7]. The hyperbolic sine gives a more uniform distribution in the immediate vicinity of the minimum spacing, and thus has less error in this region, but the hyperbolic tangent has the better overall distribution. The important point is that the spacing must not be allowed to change too rapidly in high gradient regions. After some testing, it was decided to use the hyperbolic tangent with a non-uniform grid extending 7.5, 5 and 6.5 units upstream, downstream and sideways from the body, respectively. Beyond that the grid distribution was made uniform with a cell size of about 0.7 length units.

For accurate calculations, the size of the cells adjacent to the cylinder should be sufficiently small. Wall distances for the near-wall node in between 0.001 and 0.005 units were investigated. For most of the results in this paper, the value 0.004 was used. Decreasing it to 0.001 gave negligible changes in the results.

Influence of Domain Size

It is well known that the size of the calculation domain may have a great influence on the results, especially for bluff-body flows. For example, at $Re = 100$, the sizes used by Kelkar & Patankar[3] ($X_u = 4$, $X_d = 9$, $B = 1/7$) and Franke & Rodi[2] ($X_u = 4.5$, $X_d = 14.5$, $B = 1/12$) were calculated on using the present method. It was found that the RMS lift decreased by 10% when going from the smaller to the larger domain.

Upstream and Downstream Extents. The influence of X_u was studied separately for $X_d = 14.9$ and $B = 7\%$ ($Re = 100$, QUICK). When increasing from $X_u = 7.5$ to $X_u = 11.1$ the RMS lift decreased by 9.3% (frontal pressure coefficient $C_{p,f}$ decreased 3.0%). A further increase up to $X_u = 18.3$ gave negligible changes (less than 1%). Thus $X_u = 11.1$ was found to be an appro-
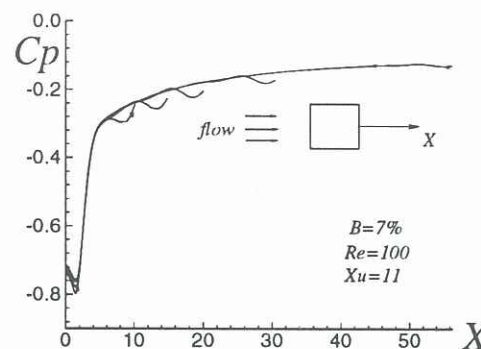
priate value.

In Table 1 and Fig. 2 the influence of the downstream extent is depicted. These results indicate that in order to obtain results independent of the outlet, the extent of the calculation domain downstream of the cylinder must be as large as $X_d = 30$. A further increase to $X_d = 56.3$ did not have any effect on the quantities listed in Table 1. Please note that the RMS lift for the case at $X_d = 14.9$ was about 12% higher than the limiting value at sufficiently large X_d. As evident from Fig. 2 the outlet boundary created some unphysical disturbances on the upstream flow. This is believed to be an effect of the Neumann conditions used at the outlet. However, when X_d is chosen large enough these effects are damped out and do not affect the flow around the body. Other boundary conditions which allow for a smoother discharge of the vortex street will be tested in the future.

Blockage. In the present work the upper and lower boundaries are treated as friction-free walls, i.e symmetry boundaries. At blockages less than 3%, when using the third-order QUICK scheme, which is unbounded, the calculations exhibited unphysical oscillations. For this reason the more stable, bounded, second-order Van Leer scheme was used also, see Table 3. The comparison between the two schemes, revealed, see Fig. 3, that the Strouhal number was quite sensitive to the type of scheme. In both cases, however, the Strouhal number showed an increase with increasing blockage (decreasing H). At these relatively low blockages, this behaviour is similar to what normally is found at much higher Reynolds numbers (in turbulent flow) where the Strouhal number is more or less independent of Reynolds number. The blockage effect could then be explained by an effective increase in the oncoming velocity. Since Strouhal number as well as force and pressure coefficients have velocity in the denominator the velocity which is actually scaled with would be too low at a non-zero blockage. In this case at $Re = 100$, there is also a relatively strong influence of the Reynolds number where the Strouhal number increases rapidly with Re (Fig. 6). The concept of an effective increase in the oncoming velocity, i.e. in the Reynolds number, would then add to the above direct effect. At this Re, the difference in level between the two schemes might be explained by the fact that the Van Leer scheme, for an identical grid, has more numerical diffusion, i.e. a higher effective viscosity, than

TABLE 1. EFFECT OF DOWNSTREAM EXTENT FOR $Re = 100$, $X_u = 11.1$, $B = 7\%$ AND QUICK SCHEME.

X_d	St	C_D	C_{D_p}	$C_{p,f}$	$C_{L'}$	$C_{D'}$	$-C_{p,tb}$	$-C_{pb}$	C_{ps}	L_r
10.2	.150	1.503	1.454	.703	.082	.0059	1.151	.735	1.027	1.90
14.9	.150	1.486	1.439	.705	.145	.0036	1.137	.723	1.027	2.08
20.0	.148	1.478	1.433	.706	.135	.0022	1.127	.714	1.027	2.20
30.4	.149	1.483	1.436	.706	.129	.0022	1.129	.715	1.027	2.18
56.3	.149	1.483	1.436	.706	.129	.0022	1.129	.715	1.027	2.18

TABLE 2. EFFECT OF BLOCKAGE FOR $Re = 100$, $X_d = 22.65$, $X_u = 18.3$ AND VAN LEER SCHEME.

B	St	C_D	C_{D_p}	$C_{p,f}$	$C_{L'}$	$C_{D'}$	$C_{p,tb}$	C_{pb}	C_{ps}	L_r
7.0	.142	1.466	1.425	.719	.127	.0023	1.106	.697	1.026	2.34
5.0	.139	1.423	1.382	.729	.130	.0025	1.042	.644	1.028	2.30
3.7	.136	1.401	1.360	.732	.129	.0029	1.006	.613	1.033	2.32
2.0	.135	1.390	1.348	.742	.122	.0044	0.971	.585	1.045	2.30
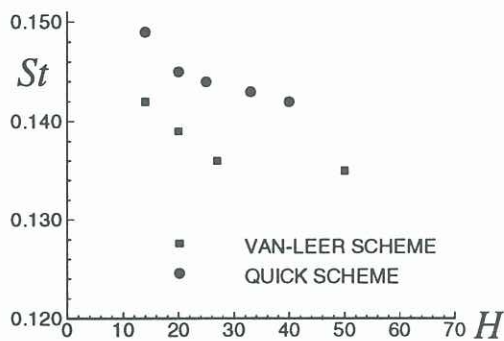
FIG. 3. THE EFFECT OF BLOCKAGE ($B = 1/H$) ON STROUHAL NUMBER.

the QUICK scheme.

Influence of Reynolds Number

In Table 3 the results at various Reynolds numbers are given ($B = 5\%$, grid 128×86). Up to Reynolds number of 50, the flow is steady (see Fig.4). Between Reynolds number of 50 and 55, the first effects of instabilities appear, which causes vortex shedding, and the flow becomes unsteady. Thus the critical Reynolds number is between 50 and 55, which is in agreement with the value of 53 found from a numerical stability analysis by Kelkar and Patankar[3].

At Reynolds numbers 55 to 75, four distinctive time phases could be identified - the first was the transient start-up phase with a sharp drop in the drag coefficient, the second phase was an interval with symmetrical flow at a low constant level of C_D which eventually was followed by the transitional phase leading to the final fully developed vortex shedding phase, see Figs. 4,5. At higher Re, i.e. at $Re > 75$ (approx.), the plateau-phase at low C_D disappeared; the transition to fully developed flow then was initiatated immediately after passing through a minimum in C_D, see Fig. 5 ($Re = 200$). The relative increase in C_D from this minimum value up the fully developed state increased with increasing Re, the increase being about 20% at $Re = 250$. For all cases, the fully developed state could be described with a single well-defined shedding frequency.

In fully developed flow, the frictional contribution to the drag was positive up to $Re = 125$ and beyond that it was negative (friction drag coefficients can be calculated from Table 3 as $C_D - C_{D_p}$). Instantaneous streamlines revealed that the separation, in fully developed flow, occurred predominantly from the rear corners at $Re \le 125$ and predominantly from the upstream corners, as the vortex shedding became more powerful, at higher Re. When separation is located at the upstream corners the flow in the separation bubble creates a near-wall flow which is directed upstream. With increasing strength of the shedding process this effect presumably becomes more pronounced.

Due to increasing viscous effects, the stagnation pressure coefficient C_{ps} increases with decreasing Reynolds number ("Barker effect"). The calculated values in Table 3 varied approximately as $1 + C/Re$ where $C = 4.2 \pm 0.6$.

In Fig. 6 the present values of C_D and St vs. Reynolds number are shown together results of other investigations. The present results for C_D show good agreement by experimental result as given in Okajima[6]. As regards previous numerical results the agreement was only of a qualitative nature. At these Re, it is suggested that the relatively strong sensitivity to various numerical parameters as well as the blockage, as demonstrated in this paper, make a significant contribution to the discrepancies in absolute levels.

CONCLUSIONS

Numerical calculations of vortex shedding past a square cylinder, at $Re = 45 - 250$ (at 5% blockage), have been reported. The onset of vortex shedding was predicted in between $Re = 50$ and $Re = 55$. The fully developed flow at $Re \ge 55$ exhibited a well-defined vortex shedding frequency. When using the RMS lift coefficient as an indicator the strong sensitivity to various numerical parameters was demonstrated. Recommendations for the required size of the domain, grid distribution, time step and spatial resolution in the near-body region are given ($Re = 100$). The blockage effect at $Re = 100$ could qualitatively be described as an effective increase in the oncoming free stream velocity.

520

TABLE 3. EFFECTS OF REYNOLDS NUMBER FOR $B = 5\%$, $X_u = 11.1$, $X_d = 25.2$ AND QUICK SCHEME.

| Re	St	C_D	C_{D_p}	$C_{p,f}$	$C_{L'}$	$C_{D'}$	$-C_{p,tb}$	$-C_{pb}$	C_{ps}	L_r
45	-	1.672	1.461	.868	-	-	.947	.558	1.079	3.18
50	-	1.605	1.424	.849	-	-	.936	.546	1.073	3.55
55	.120	1.600	1.437	.826	.054	.0003	.978	.583	1.066	2.91
60	.123	1.573	1.429	.808	.064	.0006	.992	.595	1.061	2.57
75	.133	1.509	1.412	.769	.087	.0011	1.022	.619	1.057	2.48
100	.145	1.444	1.398	.726	.130	.0019	1.063	.623	1.048	2.22
125	.155	1.416	1.404	.698	.155	.0035	1.092	.694	1.034	2.05
150	.161	1.408	1.420	.681	.177	.0061	1.129	.730	1.028	1.89
175	.165	1.412	1.440	.669	.202	.0089	1.155	.764	1.025	1.78
200	.165	1.424	1.464	.662	.240	.0121	1.173	.796	1.023	1.72
225	.161	1.434	1.483	.659	.298	.0146	1.171	.817	1.020	1.72
250	.151	1.449	1.501	.663	.375	.0162	1.157	.832	1.019	1.77
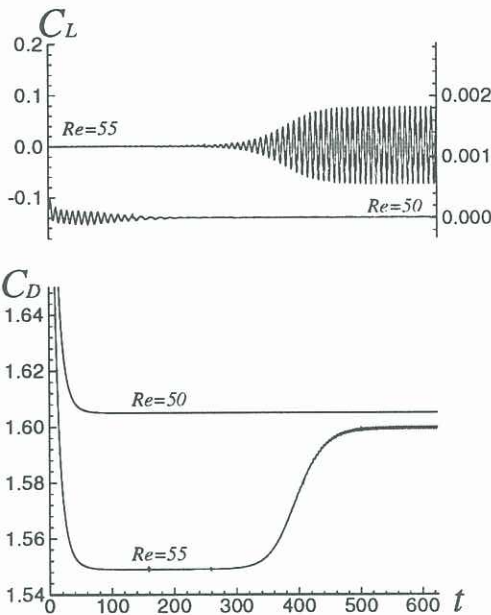
FIG. 4. LIFT AND DRAG COEFFICIENTS, WITH ($Re = 55$) AND WITHOUT VORTEX SHEDDING
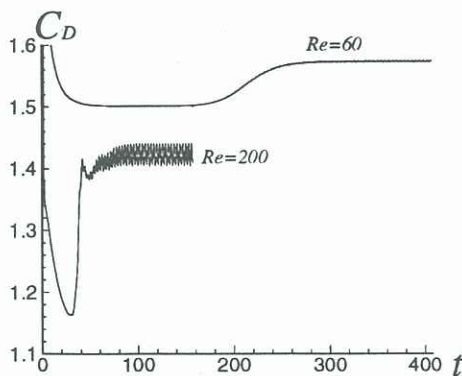
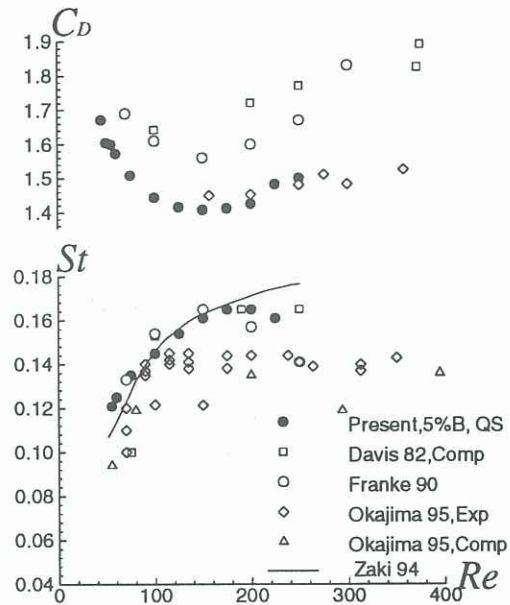FIG. 5. TIME EVOLUTIONS OF THE TOTAL DRAG COEFFICIENT.

FIG. 6. COMPARISON BETWEEN COMPUTED AND MEASURED VALUES OF DRAG COEFFICIENT AND STROUHAL NUMBER.

REFERENCES

1. Davis, R.W. & Moore, E.F. 1982. *J. Fluid Mech.*, **116**, 475.

2. Franke, R., Rodi, W. & Schönung, B. 1990 *J. Wind Engng. Ind. Aero.*, **35**, 237.

3. Kelkar, K.M. & Patankar, E.F. 1992 *Int. J. Num. Methods in Fluids*, **14**, 327.

4. Okajima, A. 1982 *J. Fluid Mech.*, **123**, 379.

5. Okajima, A., Nagahisa, T. & Rokugoh, A. 1990 *JSME Int. J., Ser. II*, **33:4**, 702.

6. Okajima, A. 1995 In Proc. *6th Int. Conf. Flow-Induced Vibration*, London/United Kingdom, April 1995, Ed. P.W. Bearman, Balkema, Rotterdam.

7. Thompson, J.E., Warsi, Z.U.A & Mastin, C.W. 1985 *Numerical Grid Generation, Foundations and Applications*, North-Holland.

8. Zaki, T.G., Sen, M. & Gad-el-Hak, M. 1994 *J. Fluids and Structures*, **8**, 555.